



Ordering transition of gases adsorbed on a C₆₀ surface: Monte Carlo simulations and lattice-gas models

Silvina M. Gatica,^{1,*} Milen K. Kostov,^{2,†} and Milton W. Cole^{3,‡}

¹*Department of Physics and Astronomy, Howard University, 2355 Sixth Street, NW, Washington, DC 20059, USA*

²*Department of Chemical and Biomedical Engineering, FAMU-FSU College of Engineering, Florida State University, Tallahassee, Florida 32310-6046, USA*

³*Department of Physics, Pennsylvania State University, 104 Davey Laboratory, University Park, Pennsylvania 16802, USA*

(Received 9 May 2008; revised manuscript received 30 July 2008; published 12 November 2008)

A monolayer of C₆₀ molecules on a flat surface provides an unusual substrate for the adsorption of simple gases. Both the lattice constant and the corrugation are larger than is typical of most traditional surfaces. These differences give rise to different phenomena, such as unusual commensurate phases. This paper discusses the ordering transition of various gases corresponding to the filling of the honeycomb array of threefold coordinated hollow sites located between C₆₀ molecules. That transition is investigated with Monte Carlo simulations and analytical (lattice-gas) models. The value of the resulting transition temperature (T_c) depends on the form assumed for the long-range interaction and the role of many-body effects, i.e., screening, due to gas molecules' close proximity to the C₆₀ layer. The effect of three-body interactions is found to be large in all cases considered.

DOI: [10.1103/PhysRevB.78.205417](https://doi.org/10.1103/PhysRevB.78.205417)

PACS number(s): 68.43.Fg, 61.48.-c, 68.35.bp, 64.60.De

I. INTRODUCTION

Interest in fullerenes has led to many studies of adsorption on carbon nanotubes.¹⁻⁵ There have also been a number of studies of gas adsorption on various forms of C₆₀ including individual buckyball molecules,⁶⁻⁸ C₆₀ monolayers,⁹⁻¹² and the bulk C₆₀ (fullerite) crystal.¹³⁻¹⁵ In the case of nanotubes, the small carbon spacing (~ 1.4 Å) implies that the corrugation—the lateral variation in the adsorption potential—is relatively small. For that reason, as well as computational simplicity, this corrugation has been omitted completely from many, but not all, theoretical studies of adsorption on nanotubes and buckyballs.

Gas adsorption on a layer of buckyballs involves *two* kinds of corrugation. One is that associated with the small C-C spacing, which is very similar to that found on nanotubes. The other corrugation is due to the large size of the buckyballs—effects of which include a large lattice constant and a significant periodic potential experienced by an adsorbate. The consequence of this potential is the existence of observable commensurate phases for various gases. The present paper explores the first commensurate phase to appear with increasing pressure of a gas of small physisorbed molecules. This phase is the ground state of this adsorption system in which each molecule is surrounded by three buckyballs (see Fig. 1). It has been observed in both LEED studies and adsorption isotherms, both experimental and simulated.⁹⁻¹¹ However, the ordering transition associated with the appearance of the molecules at these sites has not yet been observed or predicted. A similar transition was investigated some time ago by the group of Vilches¹⁶ that involves adsorbed gases on the surface of graphite “preplated” with a monolayer of Kr. These commensurate phases exhibit the same symmetry as that found in the buckyball problem, but the lattice constant is much larger and the transition temperature is much lower in the latter case because the Xe diameter is less than half that of C₆₀.

This paper presents computer simulations of the adsorption of Xe on a monolayer C₆₀ film. The resulting isotherms, coverage vs pressure, exhibit a low-pressure, low-temperature step corresponding to the filling of these sites to which the adsorbate is strongly bound. The transition of interest involves the interactions between these adsorbed molecules. The critical temperature T_c for this transition is proportional to this interaction strength as is known from lattice-gas (LG) models of adsorption. In the simplest treatment, the only role of the C₆₀ molecules is to provide the sites used in the lattice-gas description. In a more elaborate exploration, the C₆₀ alters the adsorbate-adsorbate interactions. While the latter is investigated here, one complication is omitted completely—the dynamics of the substrate. This is justified by the fact that the temperatures are so low that the relevant C₆₀ motions are small.

We consider here a variety of interaction models in order to explore the various effects that determine T_c . The resulting values of T_c vary by more than a factor of two for a given adsorbate, depending on the choice of model. Experimental observation of the transition will provide valuable information about these interactions.

II. SIMULATIONS WITH LENNARD-JONES INTERACTIONS

We have used grand canonical Monte Carlo simulations to predict the adsorption behavior of Xe on the C₆₀ surface. The method, identical to that used in our previous study of this problem,¹⁰ requires two input potentials. One is the Xe-Xe interaction, for which we have used the venerable Lennard-Jones (LJ) interaction, with parameters $\sigma=4.1$ Å and $\epsilon/k_B=221$ K, respectively. The other is the Xe-C₆₀ interaction, which we take to have the form

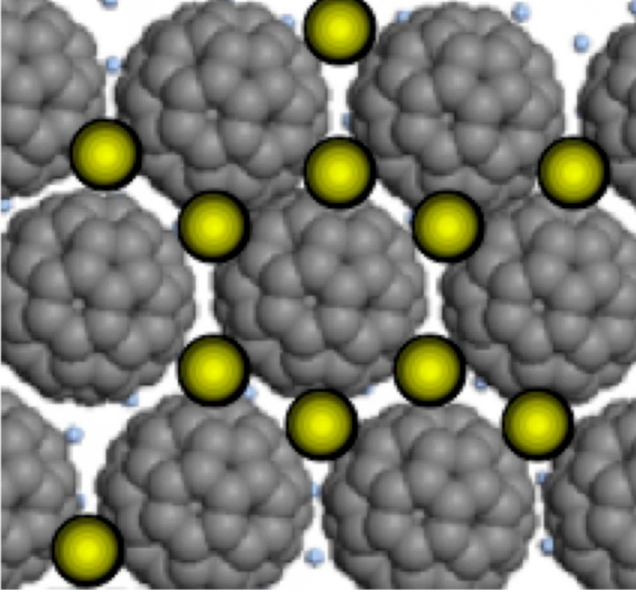


FIG. 1. (Color online) Schematic view of the buckyballs (gray) with some occupied adsorption sites (yellow circles). These sites are located 0.44 nm above the plane containing the centers of the buckyballs.

$$V_{C_{60}}(r) = 4\pi nR\epsilon_{gs} \frac{1}{r} \left\{ \frac{\sigma_{gs}^{12}}{5} \left[\frac{1}{(r-R)^{10}} - \frac{1}{(r+R)^{10}} \right] - \frac{\sigma_{gs}^6}{2} \left[\frac{1}{(r-R)^4} - \frac{1}{(r+R)^4} \right] \right\}. \quad (1)$$

Here, $R=3.55 \text{ \AA}$, $\sigma_{gs}=3.75 \text{ \AA}$, and $\epsilon_{gs}/k_B=78.7 \text{ K}$ are the Xe- C_{60} LJ interaction parameters used in previous work. This interaction is derived¹⁵ by integrating the two-body potential over the buckyball surface, which is taken to be a two-dimensional continuum of carbon with atomic density $0.38/\text{\AA}^2$. This continuum representation of the buckyball's adsorption potential is an adequate approximation found experimentally to be accurate for the case of nanotube adsorption.¹ Possible improvements of the model to include corrugation would assume transferability of experience with adsorption on graphite, for which the magnitude of the corrugation remains ambiguous in spite of 50 years of study of that problem.¹⁷

Figure 2 shows the resulting isotherms as a function of temperature. The control parameter is the chemical potential, μ , which is a monotonic function of pressure, P , given for an ideal gas by the relation $\beta\mu = \ln[\beta P \lambda^3]$. Here $\beta^{-1}=k_B T$ and λ is the de Broglie thermal wavelength. The ideal-gas assumption is well satisfied in the present regime of P and T .

Below about 35 K, the observed phases, depending on μ , are either a low-density gas or a high-density "condensed" phase in which nearly all sites are occupied. There is a vertical step that separates these two regimes of coverage corresponding to a pressure (chemical potential) at which two-phase coexistence occurs. Near and above 40 K, instead, the curves are rounded, indicating that the system is within the hypercritical regime. We estimate the critical temperature from these simulations to be $(T_c)_{sim}=35 \pm 5 \text{ K}$.

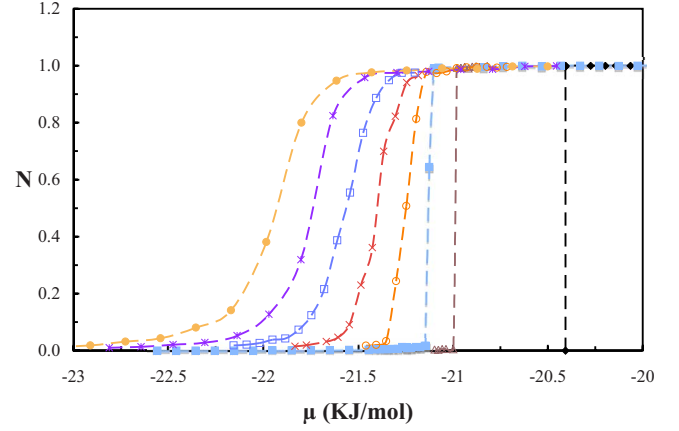


FIG. 2. (Color online) Fractions of threefold sites that are occupied by Xe atoms as a function of chemical potential and temperature. From right to left, the simulated temperatures are 23, 25, 30, 35, 40, 45, 50, and 55 K, respectively.

Quite careful investigation (using simulations) of the transition might be warranted except for the fact that this observed behavior is characteristic of the much-studied LG transition, for which the critical exponents are known to be described exactly by the two-dimensional Ising model.¹⁸ The LG approach is commonly used to describe the liquid-vapor transition even though the model's discretization oversimplifies the physics of these fluid phases. The model's validity in describing critical behavior is a result of universality because the dimensionality of the order parameter is one for both the LG and the realistic condensation cases. The application of the LG model is somewhat more appropriate for the present application than for bulk condensation since the artifact of the lattice structure is a reality for the adsorption problem. Indeed, the potential localizing the atoms at these sites on C_{60} is much larger than is encountered in most adsorption problems.

III. ISING-MODEL INVESTIGATION OF T_c

The appropriate model for this system is the Ising model on a honeycomb lattice. An exact solution for the critical temperature is given by the formula^{19,20}

$$(k_B T_c / J)_{\text{honey}} = 2 / \ln[2 + 3^{1/2}] \approx 1.519. \quad (2)$$

Here J is the (ferromagnetic) exchange coupling within this model, which includes only the nearest-neighbor interaction energy $|V|$. The factor ~ 1.52 is approximately one half of the mean-field value 3.0, which is equal to the number of nearest neighbors. In the transformation from the LG model to the Ising model, the relationship between parameter values is $J = -V/4$. In the case of Lennard-Jones interactions, the value of J might be taken to be J_{LJ} , which is derived from the pair interaction

$$V_{LJ}(r) = 4\epsilon[(\sigma/r)^{12} - (\sigma/r)^6] \sim -C_{LJ}/r^6, \quad (3)$$

$$C_{LJ} = 4\epsilon(\sigma/r)^6. \quad (4)$$

Here $r=5.8 \text{ \AA}$ is the spacing between Xe atoms in the honeycomb array. The omitted repulsive term in the right-most

TABLE I. LJ interaction parameters, σ and ε , and predicted critical temperatures [from Eq. (7a)] for gases on C_{60} . Parameters taken from Berry *et al.* (Ref. 22) or Wang and Johnson (Ref. 23), from which $C_{LJ} = 4\varepsilon\sigma^6$ is computed. Values of C_6 are from Kumar and Meath (Ref. 24) for atoms or Bruch *et al.* (Ref. 20) for molecules. Gases are listed in the order of T_c . Three-body interactions are *not* included in its determination. The three-body/two-body ratio, $-V_3/V_2$, is between particles on neighboring sites. The critical point for the bulk phase is included for comparison.

Gas	σ (Å)	ε (K)	C_{LJ} (KÅ ⁶)	C_6/C_{LJ}	T_c (K)	$-V_3/V_2$	$T_{c\text{-bulk}}$ (K)
He	2.556	10.22	1.14E4	0.89	0.11	0.62	5.21
Ne	2.749	35.60	6.15E4	0.72	0.49	7.94	44.4
H ₂	2.928	37	9.33E4	0.85	0.88	0.69	32.99
O ₂	3.58	117.5	9.89E5	0.43	4.5		154.6
Ar	3.405	119.8	7.47E5	0.60	4.9	0.52	150.7
N ₂	3.698	95.05	9.72E5	0.52	5.3		126.3
CH ₄	3.817	148.2	1.83E6	0.49	9.3		190.7
Kr	3.60	171	1.49E6	0.60	9.5	0.53	209.4
Xe	4.10	221	4.20E6	0.47	19	0.43	289.7

expression of Eq. (3) represents a 12% correction to U , and hence, J . In the simulations, of course, the complete LJ interaction was used, resulting in a value of $V_{LJ}(r) = 96.7$ K. Thus, the exchange energy is $J_{LJ} = -V_{LJ}(r)/4 \approx 24.2$ K. This results in a transition temperature [predicted by Eq. (2)] of $(T_c)_{LJ} = 37$ K. This value is close to that estimated from the simulation results of Fig. 2.

One might inquire about corrections to the model predictions arising from long-range interactions. A simple estimate of the effect of the more distant neighbors employs the following *ansatz*: an “improved” value (J') of the exchange parameter is derived from the ratio of the net interaction energy per particle V_{total} for the fully occupied lattice to the value $(3/2)V_{LJ}(r)$ found from a model with only nearest-neighbor interactions. That is, the long-range interaction correction factor is given by

$$J'/J = 2V_{\text{total}}/[3V_{LJ}(r)]. \quad (5)$$

We find (from a lattice sum over the honeycomb array) that the right-hand side is equal to 1.14 so that our corrected estimate is $(T_c)_{LJ, \text{corrected}} \sim 42$ K. This value is higher than the simulation results appearing in Fig. 2.

The preceding estimate of T_c is an improved version of the original prediction based on the LJ potential. However, this value needs to be further modified because of the inadequacy of the LJ form of the interaction. To be specific, the free-space interaction between atoms assumes the general form $V(r) \sim -C_6/r^6$ at large separation r , where C_6 is the van der Waals interaction coefficient (the value of which is known, within a few percent for the inert gases).^{21,22} The theoretical value of C_6 is significantly less than the value (C_{LJ}) computed above from the LJ functional form,

$$C_{LJ} = 4\varepsilon\sigma^6. \quad (6)$$

The ratio C_{LJ}/C_6 is about a factor of two for Xe as seen in Table I. This inadequacy of the asymptotic form of the LJ potential reflects the fact that its parameters were chosen to

fit the virial coefficient and other data, thus emphasizing accuracy of the fit near the minimum of the potential at the expense of accuracy at large separation.

In order to compute the resulting T_c with the corrected interaction, we incorporate the revised values of the asymptotic coefficient in a straightforward rescaling of the previous result. Including all of the factors mentioned above, the resulting expression is

$$k_B T_c = 1.14[1.52(C_6/C_{LJ})]V_{LJ}(r)/4 = 0.43(C_6/C_{LJ})|V_{LJ}(r)|. \quad (7a)$$

Table I presents values of the predicted critical temperatures for a number of simple gases. We note in passing that a slightly simpler expression would result if the repulsive part of the interaction were neglected,

$$(k_B T_c)' = 0.43C_6/r^6. \quad (7b)$$

The difference between Eqs. (7a) and (7b) is the inclusion of the repulsion in the former equation, which should therefore be more accurate. The difference is small for the gases shown in the table with a maximum 12% effect for Xe. [The ratio of the repulsion to the attraction for a LJ gas is the factor $(\sigma/r)^6$, which is larger for Xe than for the other gases.]

IV. THREE-BODY CORRECTION TO THE Xe-Xe INTERACTION

The interaction between Xe atoms is modified by the presence of the substrate. This many-body correction will further alter the predicted value of T_c . For semi-infinite surfaces within the continuum approximation, an expression obtained by McLachlan²⁵ was used to evaluate this correction for physisorbed noble gases. In other cases, the three-body Axilrod-Teller-Muto [or “triple-dipole” (DDD)] dispersion energy has been used to evaluate the substrate-mediated dispersion energy.^{26–29} This energy is the nonadditive dispersion energy arising in third-order perturbation theory from the interactions of fluctuating dipole moments on the two adatoms and one carbon atom.

The DDD energy $V_{AAC}^{(3)}$ at fixed adatom separation $|\vec{r}_i - \vec{r}_j| = 5.8 \text{ \AA}$ is given by a sum over carbon atoms' positions

$$V_{AAC}^{(3)}(\mathbf{r}_i, \mathbf{r}_j) = \sum_k U^{(3)}(\mathbf{r}_i, \mathbf{r}_j, \mathbf{r}_k). \quad (8)$$

Here \vec{r}_k is the position of the k th carbon atom on the buckyball surface and $U_{AAC}^{(3)}$ is its DDD interaction with adatoms at \vec{r}_i and \vec{r}_j . A simple result for the Axilrod-Teller-Muto interaction $U_{AAC}^{(3)}$ holds for isotropic oscillators at large separations,

$$U_{AAC}^{(3)} = \nu_{AAC} \frac{3 \cos \theta_i \cos \theta_j \cos \theta_k + 1}{r_{ij}^3 r_{ik}^3 r_{jk}^3}. \quad (9)$$

Here ν_{AAC} is the DDD coefficient; r_{ij} , r_{ik} , and r_{jk} are the interatomic distances in a given triplet; while θ_i , θ_j , and θ_k are the internal angles of the triangle formed by the atoms i , j , and k . The sign of the DDD energy depends on the geometry of the triangle formed by the three atoms. It is positive for acute triangles, while for most obtuse triangles it is negative so that there is significant cancellation among terms of opposite signs.

The strength coefficient ν_{AAC} can be estimated with a Drude-type or London-type single energy approximation to the atomic spectra,

$$\nu_{AAC} = \frac{3\alpha_A^2 \alpha_C E_C E_A (E_C + 2E_A)}{4(E_A + E_C)^2}. \quad (10)$$

Here α_A is the static polarizability of a Xe atom, and α_C is the static polarizability of a carbon atom on the C_{60} surface—the experimental value of 1.275 \AA^3 taken from Antoine *et al.*³⁰ The energies E_A and E_C are characteristic energies of the adatom and C atom, respectively. E_A is taken from Ref. 7, while E_C is approximated with the characteristic energy E_C derived for graphite, $E_C = 16.2 \text{ eV}$. The resulting dispersion constant is $\nu_{AAC} = 2002 \text{ K \AA}^9$.

For simplicity, we perform the summation of gas-surface DDD interactions [Eq. (8)] by smearing out the carbon atoms on the buckyballs' surfaces. This continuous approximation introduces an error, but the qualitative trends are expected to be accurate; in any case, we do not know the orientation of the individual buckyballs. The major contribution to the DDD dispersion energy comes from the four buckyballs adjacent to the physisorbed Xe; these four nearest-neighbor buckyballs are denoted by I and II in Fig. 3. The contribution of the next four closest buckyballs is tiny; the inclusion of these second-order C_{60} 's leads to only $\sim 0.3\%$ correction to the overall DDD energy. We consider, therefore, only the screening effect from the four neighboring C_{60} 's (Fig. 3). Under these assumptions, the net DDD contribution from four buckyballs, of radius $R = 3.55 \text{ \AA}$, takes the form

$$V_{AAC}^{(3)} = \frac{n\nu_{AAC}}{l^3 R^4} [M_I(a, b'_I, b''_I) + M_{II}(a, b'_{II}, b''_{II})], \quad (11)$$

where $n = 0.38 \text{ \AA}^{-2}$ is the surface density of carbon atoms and $l = 5.8 \text{ \AA}$ is the distance between adatoms. Here, $a = l/R$, $b'_I = b''_I = d/R$, $b'_{II} = d/R$, and $b''_{II} = 1.7d/R$ where $d = 7.28 \text{ \AA}$ is the distance from the adatom to the center of the buckyball. The parameters b'_I and b''_I reflect the relative positions of the centers of buckyballs (Fig. 3). The integrals

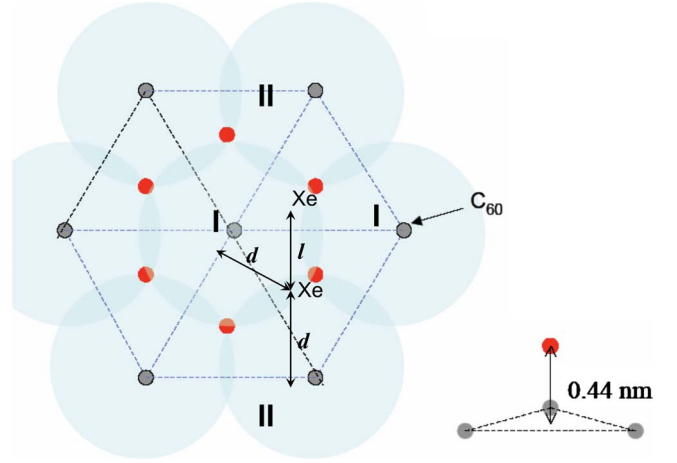


FIG. 3. (Color online) Schematic geometry depicting the three-body Xe-Xe-C interactions. The main contribution to the DDD dispersion energy comes from the four fullerenes denoted as I and II. Note that the Xe adsorption sites are located in a plane 4.4 \AA above the plane containing the buckyball centers.

$M_I(a, b'_I, b''_I)$ and $M_{II}(a, b'_{II}, b''_{II})$ are dimensionless integrals over the finite spherical surface of the four nearest-neighbor buckyballs. Numerical integration over the spherical surface is carried out using the MATHEMATICA6.0 software package.³¹

In the case of type I buckyballs, we find a strongly repulsive DDD interaction with energy $V_{AAC}(I) = 26 \text{ K}$. The geometry of type II favors the formation of more obtuse triangles, which leads to a net attractive DDD energy: $V_{AAC}(II) = -3.1 \text{ K}$. Summing these terms, the overall DDD dispersion energy is repulsive: $V_{AAC} = 22.9 \text{ K}$. Compared to the free-space pair interaction $U_{AA}^{(2)}$ at adatom separation $l = 5.8 \text{ \AA}$ ($U_{AA}^{(2)} = 53 \text{ K}$), the three-body DDD screening effect is quite large ($\sim 43\%$) such that the attraction between Xe atoms is reduced to just 57% of its free-space value.

Results for the three-body energy V_3 of other simple gases are shown in the right column of Table I—expressed as $-V_3/V_2$, which is the magnitude of the ratio of this energy to the pair energy V_2 (for particles on neighboring sites). The ratio is seen to be even larger for the other gases than for Xe, which can be explained by the closer proximity of the adsorbed species to the surrounding C atoms. The vertical locations of the adsorption sites with respect to the buckyball centers are $2.9, 3.1, 3.4, 3.8,$ and 3.9 \AA for He, Ne, H_2 , Ar, and Kr, respectively. An exceptionally large ratio [$(-V_3/V_2) \sim 8$] was found for Ne. The reason is that, for Ne, the numerator of this ratio is particularly large and the denominator is much smaller than what occurs for other gases. The numerator is large because neon's small size means that it adsorbs particularly close to the C_{60} , enhancing the three-body interaction, which varies as a very high inverse power of separation. The denominator is small because the Ne-Ne separation on the surface is large compared to neon's equilibrium spacing. We are not aware of other cases where the three-body interaction is so high. In all of these cases, one must be concerned about the role of higher-order many-body forces, which are surely not negligible if the three-body energy is so large.

We note in passing that there exists a different kind of three-body interaction present in this problem involving

three adatoms, $V_{AAA}^{(3)}$. Since three-body interactions vary as a triple product of the polarizabilities divided by the cube of the separations, which are quite large for the adatoms, this energy is small compared to the three-body energy involving the ensemble of C atoms.

V. DISCUSSION

In this paper we have addressed a low-temperature transition of gases adsorbed on a monolayer of C_{60} . The key theoretical variable determining the critical temperature is the long-range interaction between the adatoms or admolecules. This quantity is well known in the gas phase but we find that the substrate modifies this interaction and therefore the transition temperature to an extent much greater than what has been found previously for other surface transitions.

The predicted critical temperatures in Table I are observed to increase with molecular interaction, ϵ , apart from N_2 , which is slightly “out of place”; alternatively, the sequence is seen to be ordered by the σ parameter (except for O_2 and Kr). In all cases, these values of T_c are much smaller than the critical temperatures, T_{bulk} , for the bulk liquid-vapor transition. The explanation is that the surface transition temperature obeys Eq. (7b) approximately, while T_{bulk} of these gases is (within a few percent) equal to 1.25ϵ . The ratio of these expressions varies as $T_c/T_{\text{bulk}} \sim (\sigma/r)^6$, which is much smaller than 1. With appropriate prefactors inserted, one finds the ratio to be $T_c/T_{\text{bulk}} \sim 0.05$ (consistent with the tabulated values) within a few percent.

The tabulated predictions of T_c do not include the effects of three-body interactions. These have been found to yield substantial repulsive interactions as was found to be the case in our previous study of adsorption on carbon nanotubes.²⁷ Where these interactions are included and higher-order interactions are negligible, the critical temperature would be reduced from the tabulated value by a factor of $1 + V_3/V_2$. The problem with making quantitative predictions based on these contributions is that large three-body interactions imply that higher-order many-body interactions are likely to be important. We intend in the future to investigate such higher-order terms using the so-called “coupled-dipole method.”³²

Because the predicted transition temperatures are so low, observing these transitions requires experimentalists to explore temperature regimes about one tenth of the bulk triple temperatures. This means that the vapor pressures are low and equilibrium will be slow. Interestingly, it may be the case that the most feasible system is He, in spite of its low value of T_c , since its quantum mobility will facilitate equilibration.

We expect that quantum effects should not alter the T_c predictions significantly since even the He atoms are highly localized near the adsorption sites by the strongly attractive potentials there.

At this point we note that He on graphite exhibits a much-studied commensurate phase—the $\sqrt{3} \times \sqrt{3}R30^\circ$ phase.^{20,33} This phase persists to quite high temperature (for He), ~ 3 K, essentially independent of isotopic species. Its transition and that of the analogous H_2 phase,³³ near 20 K, are described by the three-state Potts model rather than the Ising model.^{34–36} The reason is that this ordered phase can occupy any one of three equivalent sublattices since nearest-neighbor hexagons are not simultaneously occupied on graphite due to the mutual repulsive interaction. As mentioned in Sec. I, a somewhat similar transition was investigated some time ago by Tejwani *et al.*¹⁶ In their study, He was adsorbed on the surface of graphite prepleated with a monolayer of Kr. The latter corresponds to a transition to a $(1 \times 1)(1/2)$ structure, which is the ground state of the system; there, only half of the possible sites are occupied in the ordered state since neighboring sites are too close for both to become occupied. In our system, instead, the ground state is a fully occupied hexagonal array as shown in Fig. 1, while the critical coverage involves a triangular array with half of the sites occupied. A wide variety of other commensurate phases and transitions between them have been seen for other adsorbed gases.^{20,33,37}

Many commensurate phases have been explored by methods other than isotherms. Direct observation with scanning tunnel microscopy (STM) is the most straightforward technique. Low-energy electron diffraction (LEED) and other diffractive techniques have the shortcoming that the phase of interest has the same symmetry as that of the C_{60} lattice. However, the critical point should be discernible because of the critical opalescence manifested in the scattering pattern.

ACKNOWLEDGMENTS

This research was supported by the NSF under Grant No. DMR-0505160, the DOE under Grant No. DE-FG02-07ER46414, and the Petroleum Research Fund under Grant No. 47213-G5. This research used resources of the National Energy Research Scientific Computing Center, which is supported by the Office of Science of the U.S. Department of Energy under Contract No. DE-AC02-05CH11231. We are grateful to Renee Diehl, Ted Einstein, Jim Gunton, Jackie Krim, Oscar Vilches, and Mike Roth for helpful comments and to Wei Jin for drawing the buckyballs in Fig. 1.

*sgatica@howard.edu

†kostov@eng.fsu.edu

‡mwc@psu.edu

¹A. D. Migone and S. Talapatra, in *Encyclopedia of Nanoscience and Nanotechnology*, edited by H. S. Nalwa (American Scientific, Los Angeles, 2004), Vol. 4, p. 749.

²*Adsorption by Carbons*, edited by E. J. Bottani and J. M. D. Tascon (Elsevier, Amsterdam, 2008).

³S. M. Gatica, M. M. Calbi, R. D. Diehl, and M. W. Cole, *J. Low Temp. Phys.* **152**, 89 (2008).

⁴S. B. Sinnott and R. Andrews, *Crit. Rev. Solid State Mater. Sci.* **26**, 145 (2001).

- ⁵A. C. Dillon and M. J. Heben, *Appl. Phys. A: Mater. Sci. Process.* **72**, 133 (2001); Giovanni Garberoglio, Michael M. DeKlavon, and J. Karl Johnson, *J. Phys. Chem. B* **110**, 1733 (2006).
- ⁶E. S. Hernández, *J. Low Temp. Phys.* **138**, 241 (2005); M. Baranco, E. S. Hernández, R. Mayol, and M. Pi, *Phys. Rev. B* **69**, 134502 (2004).
- ⁷S. A. Sartarelli, L. Szybisz, and E. Hernández, *J. Low Temp. Phys.* **138**, 979 (2005).
- ⁸J. D. Turnbull and M. Boninsegni, *Phys. Rev. B* **71**, 205421 (2005).
- ⁹R. A. Trasca, M. W. Cole, T. Coffey, and J. Krim, *Phys. Rev. E* **77**, 041603 (2008).
- ¹⁰S. M. Gatica, H. I. Li, R. A. Trasca, M. W. Cole, and R. D. Diehl, *Phys. Rev. B* **77**, 045414 (2008); S. M. Gatica, M. J. Bojan, G. Stan, and M. W. Cole, *J. Chem. Phys.* **114**, 3765 (2001).
- ¹¹H. I. Li, K. J. Hanna, J. A. Smerdon, R. D. Diehl, K. Pussi, and W. Moritz (unpublished).
- ¹²T. Coffey and J. Krim, *Phys. Rev. B* **72**, 235414 (2005).
- ¹³W. Teizer and R. B. Hallock, *J. Low Temp. Phys.* **109**, 243 (1997); W. Teizer, R. B. Hallock, and A. F. Hebard, *ibid.* **110**, 647 (1998); W. Teizer, R. B. Hallock, Q. L. Hudspeth, and A. F. Hebard, *ibid.* **113**, 453 (1998).
- ¹⁴C. P. Chen, S. Mehta, L. P. Fu, A. Petrou, F. M. Gasparini, and A. Hebard, *Phys. Rev. Lett.* **75**, 1871 (1995); C. P. Chen, S. Mehta, E. A. Hoefling, S. Zelakiewicz, and F. M. Gasparini, *J. Low Temp. Phys.* **102**, 31 (1996).
- ¹⁵E. S. Hernández, M. W. Cole, and M. Boninsegni, *J. Low Temp. Phys.* **134**, 309 (2004).
- ¹⁶M. J. Tejwani, O. Ferreira, and O. E. Vilches, *Phys. Rev. Lett.* **44**, 152 (1980); O. E. Vilches, *Annu. Rev. Phys. Chem.* **31**, 463 (1980).
- ¹⁷L. W. Bruch, in *Phase Transitions in Surface Films 2*, edited by H. Taub, G. Torzo, H. J. Lauter, and S. C. Fain, Jr. (Plenum, New York, 1991), p. 67.
- ¹⁸H. K. Kim and M. H. W. Chan, *Phys. Rev. Lett.* **53**, 170 (1984).
- ¹⁹K. Husimi and I. Syozi, *Prog. Theor. Phys.* **5**, 177 (1950); B. M. McCoy and T. T. Wu, *The Two-Dimensional Ising Model* (Harvard University Press, Cambridge, MA, 1973).
- ²⁰L. W. Bruch, M. W. Cole, and E. Zaremba, *Physical Adsorption: Forces and Phenomena* (Dover, Mineola, NY, 2007); see Appendix E.
- ²¹J. M. Standard and P. R. Certain, *J. Chem. Phys.* **83**, 3002 (1985); K. T. Tang, J. P. Toennies, and C. L. Yiu, *Phys. Rev. Lett.* **74**, 1546 (1995).
- ²²R. S. Berry, S. A. Rice, and J. Ross, *Physical Chemistry* (Wiley, New York, 1980).
- ²³P. Diep and J. K. Johnson, *J. Chem. Phys.* **112**, 4465 (2000).
- ²⁴A. Kumar and W. J. Meath, *Mol. Phys.* **54**, 823 (1985).
- ²⁵A. D. McLachlan, *Mol. Phys.* **7**, 381 (1964).
- ²⁶H. Y. Kim and M. W. Cole, *Phys. Rev. B* **35**, 3990 (1987); *Surf. Sci.* **194**, 257 (1988).
- ²⁷M. K. Kostov, M. W. Cole, J. C. Lewis, P. Diep, and J. K. Johnson, *Chem. Phys. Lett.* **332**, 26 (2000).
- ²⁸M. J. Elrod and R. J. Saykally, *Chem. Rev. (Washington, D.C.)* **94**, 1975 (1994).
- ²⁹J. A. Barker, in *Simple Molecular Systems at Very High Density*, edited by A. Polian, P. Loubeyre, and N. Boccara (Plenum, New York, 1989), pp. 341–351.
- ³⁰R. Antoine, Ph. Dugourd, D. Rayane, E. Benichou, M. Broyer, F. Chandezon, and C. Guet, *J. Chem. Phys.* **110**, 9771 (1999).
- ³¹<http://www.wolfram.com>
- ³²Hye-Young Kim, J. O. Sofo, D. Velegol, M. W. Cole, and A. A. Lucas, *Langmuir* **23**, 1735 (2007).
- ³³J. G. Dash, M. Schick, and O. E. Vilches, *Surf. Sci.* **299-300**, 405 (1994); D. S. Greywall, *Phys. Rev. B* **41**, 1842 (1990); **47**, 309 (1993).
- ³⁴H. Wiechert, *Physica B* **169**, 144 (1991).
- ³⁵Fred Y. Wu, *Rev. Mod. Phys.* **54**, 235 (1982).
- ³⁶M. Bretz, *Phys. Rev. Lett.* **38**, 501 (1977).
- ³⁷L. W. Bruch, R. D. Diehl, and J. A. Venables, *Rev. Mod. Phys.* **79**, 1381 (2007).